AIP Journal of Applied Physics

Nanosecond-laser plasma-assisted ultradeep microdrilling of optically opaque and transparent solids

Stanley Paul, Sergey I. Kudryashov, Kevin Lyon, and Susan D. Allen

Citation: Journal of Applied Physics **101**, 043106 (2007); doi: 10.1063/1.2434829
View online: http://dx.doi.org/10.1063/1.2434829
View Table of Contents: http://scitation.aip.org/content/aip/journal/jap/101/4?ver=pdfcov
Published by the AIP Publishing

Nanosecond-laser plasma-assisted ultradeep microdrilling of optically opaque and transparent solids

Stanley Paul,[a] Sergey I. Kudryashov,[b] Kevin Lyon, and Susan D. Allen
Department of Chemistry and Physics, Arkansas State University, State University, Arkansas 72467-0419

(Received 24 October 2006; accepted 4 December 2006; published online 23 February 2007)

A mechanism of ultradeep (up to tens of microns per pulse, submillimeter total hole depths) plasma-assisted ablative drilling of optically opaque and transparent materials by high-power nanosecond lasers has been proposed and verified experimentally using optical transmission and contact photoacoustic techniques to measure average drilling rates per laser shot versus laser intensity at constant focusing conditions. The plots of average drilling rates versus laser intensity exhibit slopes which are in good agreement with those predicted by the proposed model and also with other experimental studies. The proposed ultradeep drilling mechanism consists of a number of stages, including ultradeep "nonthermal" energy delivery into bulk solids by the short-wavelength radiation of the hot ablative plasma, bulk heating and melting, accompanied by subsurface boiling in the melt pool, and resulting melt expulsion from the target. © *2007 American Institute of Physics*.
[DOI: 10.1063/1.2434829]

I. INTRODUCTION

The process of ultradeep (multimicron) drilling of metals, semiconductors, and dielectrics by high-power short pulse (sub- and nanosecond) laser radiation has been studied extensively and systematically in the last decade.[1–5] The most commonly accepted drilling mechanism is that the material when heated by a short laser pulse is removed by permanent expulsion of a molten material from a keyhole assisted by a recoil pressure that is generated by intense surface vaporization of the melt.[6] The expulsion process, together with surface tension or chemical effects, provides access for the incident laser radiation to melt the solid material on the bottom of the melt pool.[6,7] This mechanism can successfully explain the quasistatic removal of a few microns of molten material blown off from the keyhole and producing a rim around it,[1,3] but not the single-shot formation of nearly debris-free multimicron-deep craters for laser intensities above some characteristic threshold in the range of $1-10^2$ GW/cm^2 accompanied by expulsion of subsonic liquid jets delayed by microseconds[1,3,5] and the microsecond appearance of UV bursts from ablated surfaces.[1,3] Moreover, ultradeep crater depths of 90 and 19 μm, in Al and Si targets, respectively, cannot result from heat conduction transport which would give much shallower heat-affected zones of depths $(\chi\tau_{\mathrm{exp}})^{1/2}\sim 10$ μm (Al) or 2 μm (Si), where $\chi_{\mathrm{melt}}=0.4$ cm^2/s (Al) or 0.15 cm^2/s (Si) (Ref. 8) is the characteristic thermal diffusivities of the corresponding molten materials and $\tau_{\mathrm{exp}}\sim 1$ μs (Al) or $\tau_{\mathrm{exp}}\geqslant 0.3$ μs (Si) is the minimum jet expulsion delay time.[1,3] Also, the subsequent processes of steady-state laser heating, melting, and vaporization of these materials fail to explain the very high removal rates observed using the 50 or 3 ns laser pulses.[1,3] The vaporization front velocities would approach the longitudinal sound velocities of 5 and 8 km/s in solid Al and Si, respectively,[8] at these removal rates. There is a speculation[9] about a propagating "transparency" wave or transient bleaching in a superheated, near-critical expanding and conducting melt which arises from a thresholdlike decrease of the electron density (Mott-type transition).[10] Such a hypothesis possesses several significant drawbacks, such as the too rapid thermal expansion required to decrease the electron density to subcritical, 10^{21} cm^{-3}, in metallic melts during such transitions[11] and the actual opaque (scattering) rather than transparent nature of the microheterogeneous near-critical fluid due to numerous thermal density fluctuations.[12]

Moreover, multimicron-deep ablative craters and corresponding high drilling rates per shot have been successfully demonstrated on Cu targets even with femtosecond laser pulses at intensities $I\sim 1$ PW/cm^2.[2] In this case, surface heating and ionization of bulk metal occur through direct absorption of laser radiation in its electronic subsystem, and ballistic transport of resulting hot electrons heats the target to submicron bulk depths.[13–15] The higher the laser intensity, the shallower the craters are expected due to denser volume energy deposition, faster ablation, and stronger plasma screening, but this is not the case.[2] In contrast, at lower femtosecond laser intensities, much smaller craters and drilling rates per laser shot were observed for Si and metals.[16,17]

It was earlier noted for the nanosecond-laser ultradeep drilling regimes that a hot ablative plasma exists in near proximity to the target surface,[1–3,5] which may heat the targets directly through characteristic and continuous thermal radiation.[6,18] Radiative energy transfer from laser-induced ablative plasmas to the targets is usually considered insignificant at low laser intensities compared to thermal conductivity and direct absorption of light,[6] while only plasma shielding of the targets from incident laser radiation is usually accounted for.[3,19,20] However, at high laser intensities, such a dense (critical or supercritical) hot plasma can augment in-

[a]Electronic mail: spaul@astate.edu
[b]Author to whom correspondence should be addressed. Present address: P. N. Lebedev Physical Institute, Moscow. Electronic mails: skudryashov@astate.edu and sergeikudryashov@yahoo.com

tense laser ablation by electronic heat conduction and short-wavelength [uv, vuv, euv, or x ray depending on plasma Boltzmann temperature T_e] radiative energy transport from the hot plasma to the target surface.[6,19–22] Electronic heat conduction accompanied by a picosecond electron-phonon thermalization process[13–15] can provide only submicron-thick heat penetration depth, $(\chi\tau_{las})^{1/2} \leqslant 1$ μm, for the characteristic electronic diffusivity in metals, $\chi \approx 1$ cm^2/s,[8] and short (femtosecond, picosecond, subnanosecond) laser pulses of duration $\tau_{las} < 10^{-8}$ s. In contrast, radiative energy transport is limited only by a penetration depth δ_λ and spectral excitance $M_\lambda(T_e)$ of short-wavelength (thermal and nonthermal) plasma radiation, dependent mostly on the plasma temperature T_e for each particular wavelength λ. Short-wavelength plasma radiation has been proven to be very efficient in laser-induced plasma-assisted ablation[23] for precise micromachining of dielectrics with common visible nanosecond lasers, creating transient regions of induced absorption on dielectric surfaces via electronic excitation by short-wavelength radiation of an extrinsic ablative laser plasma, but the actual energy deposition mechanism in laser-induced plasma-assisted ablation is not yet well understood.[24]

In this study we formulate a model explaining how short-wavelength thermal radiation from an ablative surface laser-induced plasma can provide ultradeep radiative energy deposition and drilling in optically opaque and transparent solids. We verify this model using experimental data on average drilling rates per laser shot as functions of laser intensity in the range of $1-10^2$ GW/cm^2 in multishot drilling experiments measured in this work by means of optical transmission and contact photoacoustic (PA) techniques.

II. FUNDAMENTALS OF PLASMA-ASSISTED ULTRADEEP LASER DRILLING OF SOLIDS AT HIGH LASER INTENSITIES

A. Laser-plasma-matter coupling mechanism on solid surfaces at high laser intensities

The critical parameter, determining the transition from a regime of surface absorption of electromagnetic radiation in absorbing solids (typical absorption coefficients $\alpha \sim 10^4-10^6$ cm^{-1}) to that of their bulk absorption ($\alpha \ll 10^4$ cm^{-1}), is the bulk plasmon wavelength $\lambda_{pl} \sim 100$ nm characteristic of these materials,[25]

$$\lambda_{pl} = \frac{2\pi c}{e}\sqrt{\frac{m^*}{N_v}} = \frac{2\pi c}{\omega_{pl}}, \tag{1}$$

where c is the speed of light in vacuum, e is the charge of an electron, m^* is its effective mass, N_v is the effective valence-electron density, and $\omega_{pl} \sim 10^{16}$ rad/s is the characteristic bulk plasmon frequency. Both real (ε_1) and imaginary (ε_2) parts of a relative permittivity for any material change drastically at $\lambda \leqslant \lambda_{pl}$,

$$\varepsilon_1 = n^2 - k^2 = 1 - \frac{\omega_{pl}{}^2\tau^2}{1+\omega^2\tau^2} \approx 1 - \frac{\lambda^2}{\lambda_{pl}{}^2} \approx 1,$$

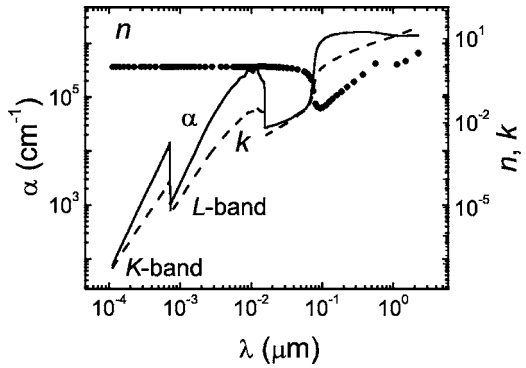

FIG. 1. Spectral dependences of refraction (n) and extinction (k) indices and absorption (α) coefficient of Al (after Ref. 25).

$$\varepsilon_2 = 2nk = \frac{\omega_{pl}{}^2\tau}{\omega(1+\omega^2\tau^2)} \approx \frac{\lambda^3}{(2\pi c\tau)\lambda_{pl}{}^2}, \tag{2}$$

where n and k are refractive index and extinction coefficient, respectively, ω is the frequency of incident radiation, and τ is the momentum relaxation time for carriers. For a radiation wavelength much shorter than the bulk plasmon wavelength, i.e., when $\lambda \ll \lambda_{pl} \ll c\tau$, the refractive index $n \approx 1$ and the extinction coefficient $k \propto \lambda^3/\tau$. The absorption coefficient $\alpha_\lambda = 4\pi k/\lambda$ will exhibit an overall trend $\alpha_\lambda \propto \lambda^2/\tau$ with several small peaks representing characteristic x-ray lines. For example, for Al at the wavelengths of 10^{-3} μm$<\lambda<10^{-2}$ μm, the extinction coefficient $k \propto \lambda^3$ (Fig. 1), while in the wavelength range of 10^{-5} μm$<\lambda<10^{-3}$ μm, $k \propto \lambda^4$, with $\alpha_\lambda \propto \lambda^3$ and $\tau \propto \lambda^{-1}$.[25] Similar behavior in the short-wavelength range of the electromagnetic spectrum is demonstrated by all other materials.[25]

Such short-wavelength (hard UV or soft x ray) radiation may be produced in hot near-surface one-dimensional (1D) laser plasmas heated to the plasma temperature T_e by incident laser radiation via the *inverse bremsstrahlung* process.[21] Indeed, x-ray quanta emitted from ablative laser-induced plasmas were observed at $\lambda_{max} \sim 10^{-4}$ μm for $I \sim 10^1-10^2$ PW/cm^2 femtosecond laser pulses[26] and at $\lambda_{max} \sim 10^{-3}-10^{-4}$ μm for $I \sim 10^2-10^5$ GW/cm^2 of subnanosecond and nanosecond laser pulses.[21,22] Corresponding temperatures of 10^2-10^3 eV can be calculated using Wien's displacement law $\lambda_{max}T = 2.9\times10^3$ μm K.[27] These observations are in agreement with scaling relationships for a thermal electron energy k_BT_e in the plasma, yielding $k_BT_e \approx C_1I^{1/2}$ (Fig. 2) for subnanosecond and nanosecond laser pulses,[3,20–22,28] where k_B is Boltzmann's constant and C_1 is some numerical factor. For femtosecond laser pulses k_BT_e scales as $C_2I^{1/2}$ or $C_3I^{5/6}$ (Fig. 2) according to calculations[29] or experimental data,[26] respectively.

The importance of the radiative transfer mechanism in coupling of the laser energy to the target via ablative laser plasma during drilling of solids can be demonstrated by comparing the incident laser intensity to that of the short-wavelength plasma radiation. According to Planck's blackbody spectral radiation law,[27] the thermal emission from a 1D homogeneously heated plasma into a solid angle of 2π sr is characterized by spectral source excitance M_λ [W/(m^2 μm)],

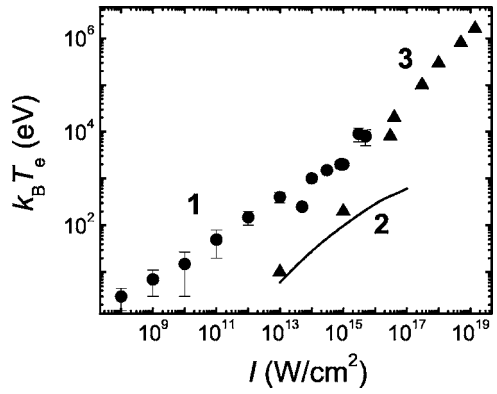

FIG. 2. Thermal electron energy $k_B T_e$ in laser plasma vs laser intensity I. Curve 1: subnanosecond and nanosecond pulses (after Refs. 21 and 22), curves 2 and 3: femtosecond pulses (after Refs. 26 and 29).

$$M_\lambda(T) = \frac{2\pi hc^2}{\lambda^5(e^{hc/\lambda kT}-1)} = \frac{3.7\times 10^8}{\lambda^5[\exp(1.44\times 10^4/\lambda T)-1]}, \tag{3}$$

where the temperature T and the wavelength λ are given in kelvins and micrometers, respectively. Integrating M_λ over the entire plasma emission spectrum at each particular T_e, one can obtain maximum intensities $I^{\mathrm{pl}}_{\max}(z=0,T_e)$ of the short-wavelength plasma radiation on the target surface $(z=0)$,

$$I^{\mathrm{pl}}_{\max}(0,T_e) = \int_0^\infty M_\lambda(0,T_e)d\lambda, \tag{4}$$

rapidly increasing at increasing laser I and the corresponding plasma T_e values. Even though effective emission times $\tau^*(T_e)$ of such superradiant plasmas are very short and rapidly decrease as $\tau^*(T_e)\propto 1/T_e^{\,2}$ in order to satisfy the energy conservation law in the form $I\tau_{\mathrm{las}}\approx I^{\mathrm{pl}}_{\max}(0,T_e)\tau^*(T_e)$ [$I\propto T_e^{\,2}$, $\tau_{\mathrm{las}}\approx$ const, and $I^{\mathrm{pl}}_{\max}\propto T_e^{\,4}$ in accordance with the Stefan-Boltzmann law,[27] so $\tau^*(T_e)\sim 1/T_e^{\,2}$], the overall effect of such radiative transfer from a hot plasma to a solid target may not be negligible.[30]

B. Plasma-assisted bulk deposition of laser energy into solids

The depth of a target irradiated by short-wavelength plasma radiation can be estimated using Wien's displacement law[27] to evaluate the "most probable wavelength" of such radiation, $\lambda_{\max}(T_e)=2.9\times 10^3\ \mu\mathrm{m\ K}/T_e$, corresponding to maximum $M_\lambda(T_e)$, and then to take the effective skin depth of the short-wavelength plasma radiation, $\delta_{\lambda\ \max}(T_e)=1/\alpha_{\lambda\ \max}(T_e)$. In doing so, one can consider plasma thermal radiation being emitted at the *single* effective wavelength $\lambda_{\max}(T_e)$ and obtain insight into the qualitative character of the laser intensity dependence of the ablation (crater) depth Z_{abl}, using a Beer's-law–like expression, $E_{\mathrm{abl}}(Z_{\mathrm{abl}})=E(0,T_e)\exp[-\alpha_{\lambda\ \max}(T_e)Z_{\mathrm{abl}}]$, for the volume energy density at the target surface, $E(z=0,T_e)=\alpha_{\lambda\ \max}(T_e)I_{\max}(0,T_e)\tau^*(T_e)$, and solving it for Z_{abl},

$$\begin{aligned} Z_{\mathrm{abl}}(I) &= \frac{1}{\alpha_{\lambda\ \max}(T_e(I))} \\ &\quad\times\ln\left[\frac{\alpha_{\lambda\ \max}(T_e(I))I_{\max}(0,T_e(I))\tau^*(T_e(I))}{E_{\mathrm{abl}}}\right] \\ &\propto I^\gamma \ln I, \end{aligned} \tag{5}$$

where the threshold volume energy density E_{abl} represents some thermal process underlying the laser ablation, e.g., melting in a case of a melt expulsion.[1–3] The exponent γ in this equation can be derived from the following considerations. As discussed above, the electron temperature in the plasma $T_e\propto I^{1/2}$ for subnanosecond and nanosecond laser pulses. Then, combining a spectral dependence of absorption coefficient $\alpha_{\lambda\ \max}\propto\lambda_{\max}(T_e)^{x(\lambda)}$ (Ref. 25) with Wien's displacement law $\lambda_{\max}\propto 1/T_e$, one can show that the exponent γ equals $x(\lambda)/2$, where $x(\lambda)$ is another exponent describing the dependence of α on λ for each particular material.

However, such a "most probable" absorption coefficient $\alpha_{\lambda\ \max}(T_e)$ for short-wavelength plasma radiation absorption in solids does not account for the asymmetry of the $M_\lambda(T_e)$ spectrum [α_λ being higher for the "red" region of the spectrum and much lower for its "blue" part (Fig. 1)]. Taking this effect into account, one can obtain the exact "mean" effective absorption coefficient $\alpha_{\mathrm{eff}}(T_e)$ or the corresponding effective mean skin depth $\delta_{\mathrm{eff}}(T_e)$,

$$\delta_{\mathrm{eff}}(T_e) = \frac{\int_0^\infty M_\lambda(0,T_e)d\lambda}{\int_0^\infty \alpha_\lambda M_\lambda(0,T_e)d\lambda}, \tag{6}$$

where only the knowledge of optical constants for the solid target of interest and plasma temperature T_e is required. If the corresponding $T_e(I)$ dependence is known, the $\delta_{\mathrm{eff}}(T_e)$ relationship can be converted to $\delta_{\mathrm{eff}}(I)=\delta_{\mathrm{eff}}(T_e(I))$.

Furthermore, the corresponding Beer's-law–like volume energy density distributions $E(z,T_e)$, described by exponents $\delta_{\lambda\ \max}$ or δ_{eff}, are not quite accurate for understanding the thermodynamic and hydrodynamic phenomena which occur during ultradeep high-power laser drilling or single-shot ablation of solids mediated by polychromatic emission of ablative surface laser plasma. More accurate spatial distributions of $E(z,T_e)$ can be obtained considering Beer's law absorption in the form $M_\lambda(z,T_e)=M_\lambda(0,T_e)\exp(-\alpha_\lambda z)$ for each particular wavelength in the plasma emission spectrum, and calculating the integral

$$E(z,T_e) = \tau^*(T_e)\int_0^\infty \alpha_\lambda M_\lambda(0,T_e)e^{-\alpha_\lambda z}d\lambda, \tag{7}$$

where z is the depth inside the target, and the effective emission time of the 1D plasma $\tau^*(T_e)\sim 1/T_e^2$ is determined directly for each set of experimental conditions from the boundary condition

$$[1-R_{\mathrm{av}}(F)]\beta(F)F=2\tau^{*}(T_e)\int_0^{\infty}M_{\lambda}(0,T_e)d\lambda, \tag{8}$$

where F is the total laser fluence incident on the target producing the ablative plasma at the very beginning of the laser pulse, $R_{\mathrm{av}}(F)$ is the corresponding reflectivity of the ablative plasma averaged over τ_{las}, and $\beta(F)$ is a fraction of the total absorbed plasma energy reemitted towards the target. The numerical factor 2 accounts for the emission of the plasma into a solid angle of 4π sr, while all temporal changes of T_e are taken into account in $\tau^{*}(T_e)$. Then, Eq. (7) can be rewritten in the final form

$$E(z,T_e)=\frac{[1-R_{\mathrm{av}}(F)]\beta(F)F\int_0^{\infty}\alpha_{\lambda}M_{\lambda}(0,T_e)e^{-\alpha_{\lambda}z}d\lambda}{\int_0^{\infty}M_{\lambda}(0,T_e)d\lambda}, \tag{9}$$

which allows for the estimation of $E(z,T_e)$ for different F and the known $R_{\mathrm{av}}(F)$, $\beta(F)$, and $T_e(I)$ dependences.

C. Removal mechanisms during ultradeep plasma-assisted laser drilling of solids

The final step in the ultradeep drilling regime—removal of ablation products—has been found to occur as expulsion of multimicrometer sized liquid droplets,[1,3,5] a size close to the characteristic radial dimensions $D\approx 30-50$ μm for ablative near-surface laser plasmas and the resulting craters,[1,3,5] providing an aspect ratio $Z_{\mathrm{abl}}/D\sim 1$ for single-shot craters.[1,3] The expulsive nature of the ultradeep drilling regime may explain the high efficiencies of material removal without considerable redeposition and the high Z_{abl} values observed.[1–3]

Moreover, high expulsion velocities, $V\sim 10^2$ m/s, measured for the ultradeep drilling and strong melt expulsion regime,[1,5] correspond to Bernoulli pressures in the molten pool, $P_B\approx\rho_{\mathrm{melt}}V^2\sim 10^2-10^3$ atm, which are on the order of magnitude of thermodynamic critical pressures $P_{\mathrm{crit}}\sim 10^3$ atm for elemental solids.[8] Surprisingly, such high pressures "blowing off" molten material build up just above the threshold for this regime (i.e., the threshold for the rapid increase of Z_{abl}), resulting in a simultaneous rapid drop of the ratio ψ of the melt volume redeposited from craters on the target surface to form a rim around the crater to the volume of the crater formed, which changes from $\psi\approx 1$ at $Z_{\mathrm{abl}}/D\ll 1$ to $\psi\approx 0.25$ at $Z_{\mathrm{abl}}/D\sim 1$ near this threshold.[3]

This change can be explained by taking into account that bulk heating of the material by the short-wavelength radiation from the 1D near-surface hot laser plasma may result not only in their ultradeep melting but also in subsurface superheating and explosive boiling of the melt pool. The subsurface superheating may be characterized by the parameter $B=(\alpha_{\lambda}\chi\Delta E_{\mathrm{boil}})/\{[1-R(I)]I\}$ (Ref. 31) or a similar parameter $b=\alpha_{\lambda}\chi/u$ (Ref. 32) (assuming $[1-R(I)]I=u\Delta E_{\mathrm{boil}}$), which shows a balance between the thermal flux $\alpha_{\lambda}\kappa\Delta E_{\mathrm{boil}}/C_p$ from hot bulk melt to its outer surface, resulting from its intense surface vaporization at the rate u, and the incoming laser flux $(1-R(I))I$, where ΔE_{boil} is the boiling (vaporization) energy density change and κ, C_p, and $R(I)$ being the thermal conductivity, isobaric heat capacity, and instantaneous reflectivity of the melt, respectively. Some would argue that the subsurface superheating effect[4,33] is not possible for large $\alpha_{\lambda}\sim 10^6$ cm^{-1} at $\lambda_{\max}(T_e(I))>\lambda_{\mathrm{pl}}$ corresponding to incident laser intensity subthreshold for the strong melt expulsion regime when $B\approx 1$ [e.g., for Si $B\approx 1$ for $\kappa\approx 0.3$ W/cm K, $\Delta E_{\mathrm{boil}}\approx 30$ kJ/cm^3, $C_{p,\mathrm{melt}}\approx 2$ J/cm^3, and $I\approx 20$ GW/cm^2 (Ref. 3)] and surface vaporization of the melt pool occurs at the nearly steady-state temperature profile in the bulk. However, this criticism is irrelevant at lower $\alpha_{\lambda}\sim 10^4$ cm^{-1} for $\lambda_{\max}(T_e(I))<\lambda_{\mathrm{pl}}$ corresponding to much higher I when $B\sim 10^{-2}\ll 1$ due to plasma-mediated ultradeep heating of these solid targets and, thus, very significant bulk superheating occurs in the melt pool at a characteristic depth of the order of α_{λ}^{-1} with negligible effect from surface evaporative cooling. The subsequent melt expulsion results from subsurface explosive boiling (boiling crisis)[4,34] in the center of the melt pool heated inhomogeneously in its radial direction because of lateral T_e inhomogeneities in the original 1D laser plasma produced by Gaussian or other similar inhomogeneous laser beams.[1,3,5] Moreover, at very high $I\sim 10^4$ GW/cm^2 corresponding to $k_BT_e\sim 10^3$ eV and $\lambda_{\max}(T_e(I))\sim 10^{-3}$ μm$\ll\lambda_{\mathrm{pl}}$, the position of a subsurface temperature maximum may lie as deep as $\alpha_{\lambda}^{-1}\sim 10-10^2$ μm (Fig. 1), corresponding to the multimicrosecond delays required to produce high vapor pressure in a subsurface bubble through explosive boiling crisis[4,34] for the expulsion of molten material and to blow off a surface "cork" of cooler melt or even solidified material. Then, the appearing subsurface hot vapor bubble can emit a burst of short-wavelength thermal radiation causing extrinsic photoelectric effect in a charge collector.[5]

III. EXPERIMENT SETUP, PROCEDURES, AND SAMPLES

In our experiments, a commercial Nd:YAG (neodium-doped yttrium aluminum garnet) nanosecond laser system (Continuum Surelite I-10, $M^2\approx 1.3$ close to a TEM_{00} mode, pulse energy $E\leqslant 60$ mJ at a wavelength $\lambda=266$ nm, pulse width τ_{LAS} [full width at half maximum (FWHM)] ≈ 10 ns, repetition rate of 1 Hz) was used to perform ultradeep drilling of materials, which were commercial silicon (Si) wafers (Motorola, thickness $D=400$ and 520 μm) and glass microscope slides (VWR Scientific, Inc., CAT. No. 48368-084, thickness $D=220$ μm). The entire experimental laser setup used is shown in Fig. 3. The number of pulses incident on the sample was controlled by a shutter. The pulse energy was varied from using a combination of color filters (Corning Glass) with different transmittivities. A beam splitter was used to reflect a part of the beam to a pyroelectric detector with digital readout (Gentec ED-500) for energy measurements in each shot. A beam expander using glass lenses $L1$ (focal length $f_1=-50$ mm) and $L2$ ($f_2=+100$ mm) was used prior to the set of filters and beam splitter to increase the beam width from 6 to 12 mm in order to fill the aperture of an imaging lens $L3$ ($f_3=25$ mm). The beam passed through

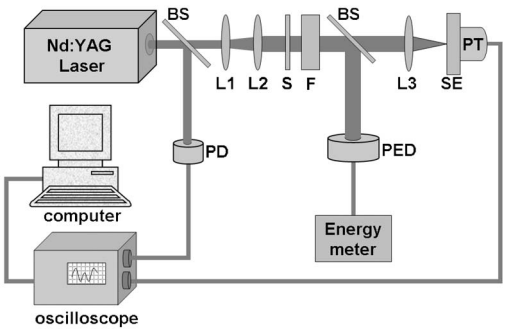

FIG. 3. Experimental laser setup (BS, beam splitter; L1, L2, and L3, lenses; S, shutter; F, filters; SE, sample; PT, photoacoustic transducer; PD, photodiode; and PED, pyroelectric detector).

the beam splitter was tightly focused onto the sample using the lens $L3$ to provide a beam waist $D_{1/e^2} \approx 40$ μm. Peak laser intensities I in these experiments were in the range of $10-10^2$ GW/cm^2, as determined using a fluence calibration procedure for single-shot surface ablation of a Si wafer at different laser energies.

PA studies were done using the same experimental setup with the Si wafers attached to the front surface of a fast acoustic transducer (5 mm thick, 1.5 mm wide $LiNbO_3$ element, flat response in 1–100 MHz range, and 3 mm protective quartz window) by means of a thin layer of vacuum grease to provide acoustic contact between the wafer and transducer.[35] The relatively large laser spot on the sample surface provided PA measurements in an acoustic mean field region. A LeCroy (Wavepro 940) storage oscilloscope triggered by a high speed silicon photodiode with 1 ns rise/fall times (Thorlabs-DET 210) was used to measure the laser pulse duration or to acquire acoustic transients (delayed by 1.1 μs in the acoustic delay line) from the transducer. A typical PA wave form, representing the first pulse of acoustic pressure $P(t)$ and its multiple subsequent reverberations in the Si wafer, is presented in Fig. 4. Within the 1 μs operating time window of the acoustic transducer (determined by the acoustic delay and subsequent reflections), the acoustic transient exhibits a prominent unipolar negative (compression)

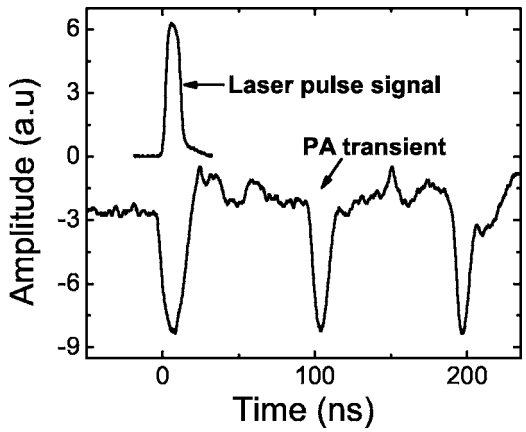

FIG. 4. Characteristic PA transient in the ultradeep drilling regime (single shot, I=62 GW/cm^2) in comparison to the laser pulse.

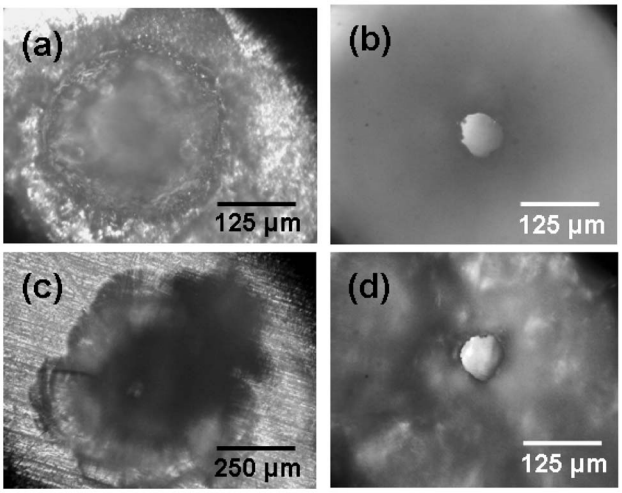

FIG. 5. Top [(a) and (c)] and rear [(b) and (d)] views of holes drilled in Si and glass samples, respectively, at $I \approx 100$ GW/cm^2.

pulse [τ_{ac}(FWHM) $\approx$ 20 ns] that qualitatively resembles the laser pulse (Fig. 4), indicating the ablative character of the corresponding acoustic generation mechanism. More detailed analysis of this mechanism will be given in a separate paper.

Average drilling rates per laser shot, $Z_{abl}=D/N_{abl}$, were obtained in this study under constant focusing conditions by measuring the number of shots N_{abl} required at the repetition pulse rate of 1 Hz to drill through the Si or glass samples at different I. N_{abl} values were obtained by multiplying the pulse rate by the time interval T_{abl} between the moment the shutter was opened and the moment when the first light comes through the drilled hole in the sample (Fig. 5), resulting in nonzero readings of the pyroelectric detector placed behind it. In the PA experiments, N_{abl} was taken when the PA signal increased dramatically, representing ablation of the residual Si or glass debris from the back side of the corresponding samples onto the thin layer of vacuum grease on the front window of the acoustic transducer by the last pulse drilled through the sample.

In order to prove that drilling rate per shot versus the number of laser shots N is nearly uniform and that the aver-

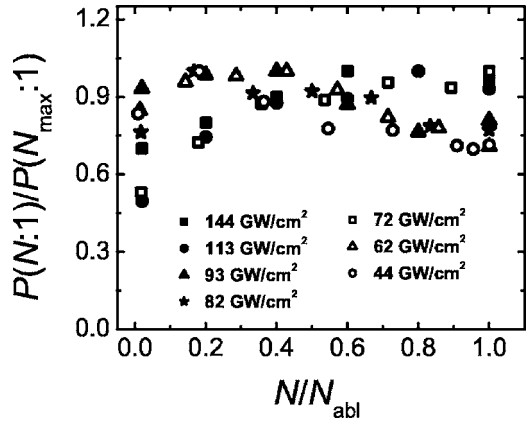

FIG. 6. Normalized pressure $P(N:1)/P(N_{max}:1)$ as a function of the normalized number of pulses, N/N_{abl} at different I values for the 400 μm thick Si sample.

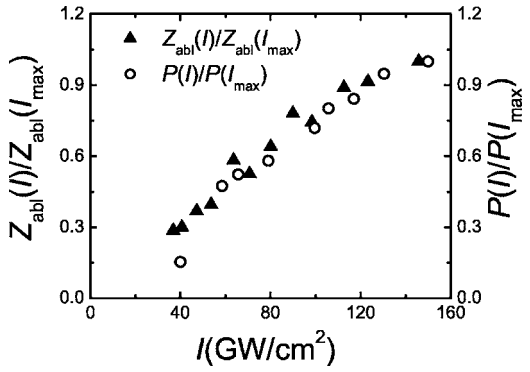

FIG. 7. Normalized acoustic pressure $P(I)/P(I_{max})$ and normalized drilling rate per shot $Z_{abl}(I)/Z_{abl}(I_{max})$ vs I for the 400 μm thick Si sample.

age Z_{abl} magnitudes are meaningful, acoustic pressure amplitudes P were measured for 400 μm thick Si wafers as a function of N (N shots on one spot, $N:1$) at constant I and presented in Fig. 6 for different I values as normalized pressures $P(N:1)/P(N_{max}:1)$, where N_{max} corresponds to the laser pulse during each pulse sequence exhibiting the maximum acoustic pressure P at the given I. As the acoustic pressure in the ablative regime represents the near-surface pressure of ablated products and laser plasma, small ($\pm 10\%$) variations of $P(N:1)/P(N_{max}:1)$ may indicate nearly uniform drilling conditions and corresponding average drilling rates per shot, Z_{abl} vs N, which differ for different I.

As an additional check of drilling rate uniformity, amplitudes of P were measured at different I after single-shot ablation of fresh spots on the surface of the 400 μm thick Si wafer and the resulting dependence $P(I)$ after normalization to the maximum pressure amplitude $P(I_{max})$ at the maximum laser intensity $I_{max} \approx 150$ GW/cm^2 used in these experiments was compared to the average drilling rate dependence $Z_{abl}(I)$, normalized to the corresponding $Z_{abl}(I_{max})$ magnitude. Good agreement of the normalized pressure $P(I)/P(I_{max})$ and drilling rate $Z_{abl}(I)/Z_{abl}(I_{max})$ curves in Fig. 7 shows that at each value of I the average drilling rate is similar to that of the first laser shot, supporting the conclusion, made on the basis of experimental data in Fig. 6, that the average drilling rate is nearly uniform.

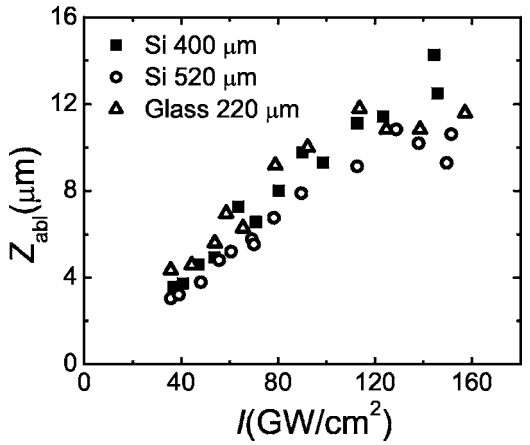

FIG. 8. Dependences of $Z_{abl}(I)$ for 400 μm (square) and 520 μm (circles) thick Si samples and the 220 μm thick glass sample (triangles).

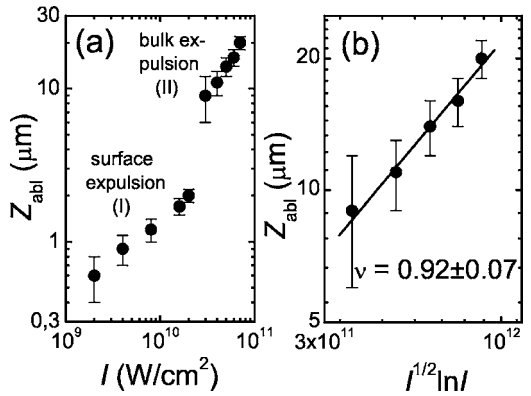

FIG. 9. (a) Crater depth Z_{abl} in Si target vs I (after Ref. 3); (b) linear fit of $Z_{abl}(I)$ in region II in (a) in double logarithmic coordinates, $\log Z_{abl} - \log[I^{1/2} \ln I]$.

IV. EXPERIMENTAL RESULTS AND DISCUSSION

The two experimental curves of average drilling rate versus laser intensity, $Z_{abl}(I)$, for Si in Fig. 8 are qualitatively consistent with the curve $Z_{abl}(I)$ representing single-shot multimicron ablation crater depth Z_{abl} in Si versus I (Fig. 9) obtained in Ref. 3 in the same intensity range and at the same laser wavelength presented in Fig. 9. The threshold intensity $I_{abl} \approx 10$ GW/cm^2 in this work is nearly two times lower than $I_{abl} \approx 20$ GW/cm^2 in Ref. 3 probably because of the dependence of T_e on τ_{las}, $T_e \propto [I\tau_{las}^{1/2}]^{1/2}$,[19,20,28] which gives for τ_{las}(FWHM) ≈ 10 ns in this work a 1.7 times lower I magnitude to heat the ablative surface laser plasma to a similar T_e as compared to the 3 ns laser pulses in Ref. 3.

Linear fits were obtained in this study for two $Z_{abl}(I)$ curves for 400 and 520 μm thick Si samples, respectively, represented in double logarithmic coordinates, $\log[Z_{abl}/\ln I] \sim \log I$, in Fig. 10. From the slope of these curves, the experimentally measured exponents γ were found to be $\gamma_{Si}^{expt} = 0.8 \pm 0.1$ ($D = 400$ μm) and $\gamma_{Si}^{expt} = 0.7 \pm 0.1$ ($D = 520$ μm), which are reasonably consistent with γ_{Si}^{theor}

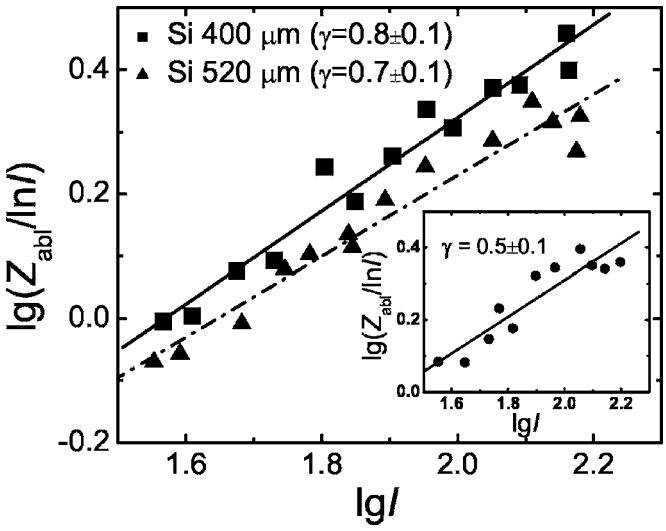

FIG. 10. Linear fits in double logarithmic coordinates $\log[Z_{abl}/\ln I] \sim \gamma \log I$ for 400 μm (squares) and 520 μm (triangles) thick Si samples and their corresponding γ slopes. Inset shows a similar fit and slope for the 220 μm thick glass sample.

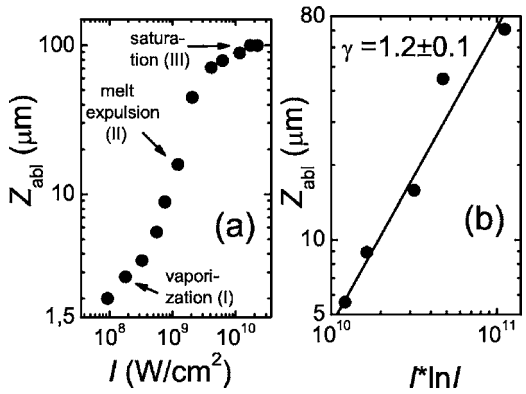

FIG. 11. (a) Crater depth Z_{abl} in Al target vs I (after Ref. 1); (b) linear fit of $Z_{abl}(I)$ in region II in double logarithmic coordinates $\log Z_{abl} - \log[I \ln I]$.

≈ 0.5 predicted from Eq. (5) for $x(\lambda) \approx 1$ in the range $10^{-3}\ \mu\text{m} < \lambda < 10^{-1}\ \mu\text{m}$.[25] Similar good agreement has been obtained between our model and the experimental results for Si given in Ref. 3 (Fig. 9). In the latter case, the experimental data fitted in the double logarithmic coordinates, $\log Z_{abl} - \nu \log[I^{1/2} \ln I]$, demonstrate $\nu = 0.92 \pm 0.07$ indicating that these data $Z_{abl}(I)$ are well described by the theoretical dependence $I^{1/2} \ln I$ predicted using Eq. (5).[18]

For the glass sample used in these experiments (see inset in Fig. 10), the exponent γ was found in the double logarithmic coordinates, $\log Z_{abl} \sim \log[I^{\gamma} \ln I]$ to be $\gamma_{glass}^{expt} = 0.5 \pm 0.1$ ($D = 220\ \mu$m) as compared to $\gamma_{FS}^{theor} \approx 0.5$ predicted from Eq. (5) for fused silica (FS) exhibiting $x(\lambda) \approx 1$ in the range of $10^{-3}\ \mu\text{m} < \lambda < 10^{-1}\ \mu\text{m}$.[25] Note that in this plasma-mediated drilling regime, ablation rates per shot at $I \leqslant 10^2$ GW/cm^2 are almost three orders of magnitude higher than for laser-induced plasma-assisted ablation at lower $I \leqslant 0.1$ GW/cm^2 at the same 266 nm laser wavelength.[36]

Finally, we have tested our model for metals using the experimental data for single-shot multimicron ablation crater depth Z_{abl} in Al versus I from Ref. 1 for the laser wavelengths of 511/578 nm and slightly lower laser intensities which still result in strong melt expulsion (Fig. 11). The double logarithmic linear fit for the data, $\log Z_{abl} \propto \log[I^{\gamma} \ln I]$, gives the value of the fitting parameter $\gamma_{Al}^{expt} = 1.2 \pm 0.1$ consistent with $\gamma_{Al}^{theor} \approx 1$ for $x(\lambda) \approx 2$ at $10^{-3}\ \mu\text{m} < \lambda < 10^{-2}\ \mu\text{m}$ (Ref. 24) predicted from Eq. (5).[18]

Thus, the experimental observations of this and other studies are consistent with the theoretical model proposed in this work to explain ultrahigh multishot drilling rates and ultradeep single-shot laser ablation craters in optically opaque and transparent solids (metals, semiconductors, and dielectrics) irradiated by high-power nanosecond-laser pulses in terms of ablative surface plasma-mediated radiative transfer of laser pulse energy to the target via short-wavelength thermal plasma radiation.

V. CONCLUSIONS

In this study we have proposed a model of ablative surface laser plasma-assisted multishot drilling or single-shot ablation of optically opaque and transparent solids irradiated by high-intensity nanosecond-laser radiation and experimentally confirmed it using laser intensity dependences of multimicron drilling rates in silicon and glass measured by optical transmission and contact photoacoustic techniques. This model also explains the experimental results of previous similar studies on silicon and aluminum.

ACKNOWLEDGMENT

The authors are grateful to the National Science Foundation for financial support (Grant No. 0218024).

[1] C. Körner, R. Mayerhofer, M. Hartmann, and H. W. Bergmann, Appl. Phys. A: Mater. Sci. Process. **63**, 123 (1996).
[2] A. Luft, U. Franz, A. Emsermann, and J. Kaspar, Appl. Phys. A: Mater. Sci. Process. **63**, 93 (1996).
[3] R. E. Russo, X. L. Mao, H. C. Liu, J. H. Yoo, and S. S. Mao, Appl. Phys. A: Mater. Sci. Process. **69**, 887 (1999); J. H. Yoo, S. H. Jeong, X. L. Mao, R. Greif, and R. E. Russo, Appl. Phys. Lett. **76**, 783 (2000).
[4] N. M. Bulgakova and A. V. Bulgakov, Appl. Phys. A: Mater. Sci. Process. **73**, 199 (2001).
[5] A. V. Pakhomov, M. S. Thompson, and D. A. Gregory, J. Phys. D **36**, 2067 (2003).
[6] C. Tix and G. Simon, Phys. Rev. E **50**, 453 (1994).
[7] D. Bäuerle, *Laser Processing and Chemistry* (Springer-Verlag, Berlin, 2000).
[8] *Fizicheskie Velichini*, edited by I. S. Grigor'ev and E. Z. Meylikhov (Energoatomizdat, Moscow, 1991).
[9] J. H. Yoo, S. H. Jeong, R. Greif, and R. E. Russo, J. Appl. Phys. **88**, 1638 (2000).
[10] V. A. Batanov, F. V. Bunkin, A. M. Prokhorov, and V. B. Fedorov, Sov. Phys. JETP **36**, 311 (1973).
[11] Ya. B. Zel'dovich and L. D. Landau, Zh. Eksp. Teor. Fiz. **14**, 32 (1944).
[12] V. P. Skripov, *Metastable Liquids* (Wiley, New York, 1974).
[13] C. Suarez, W. E. Bron, and T. Juhasz, Phys. Rev. Lett. **75**, 4536 (1995); J. Hohlfeld, J. G. Müller, S.-S. Wellershoff, and E. Matthias, Appl. Phys. B: Lasers Opt. **64**, 387 (1997).
[14] S. I. Kudryashov and V. I. Emel'yanov, JETP Lett. **73**, 666 (2001).
[15] N. M. Bulgakova, R. Stoian, A. Rosenfeld, I. V. Hertel, and E. E. B. Campbell, Phys. Rev. B **69**, 054102 (2004).
[16] S. Juodkazis, H. Okuno, N. Kujime, S. Matsuo, and H. Misawa, Appl. Phys. A: Mater. Sci. Process. **79**, 1555 (2004).
[17] G. Kamlage, T. Bauer, A. Ostendorf, and B. N. Chichkov, Appl. Phys. A: Mater. Sci. Process. **77**, 307 (2003).
[18] S. I. Kudryashov, A. V. Pakhomov, and S. D. Allen, Proc. SPIE **5713**, 508 (2005).
[19] F. Beinhorn, J. Ihlemann, K. Luther, and J. Troe, Appl. Phys. A: Mater. Sci. Process. **79**, 869 (2004).
[20] C. R. Phipps and R. W. Dreyfus, *Laser Ionization Mass Analysis* (Wiley, New York, 1993); C. P. Phipps, J. R. Luke, T. Lippert, M. Hauer, and A. Wokaun, Appl. Phys. A: Mater. Sci. Process. **79**, 1385 (2004).
[21] J. F. Ready, *Effects of High-Power Laser Radiation* (Academic, New York, 1971).
[22] L. M. Wickens, J. E. Allen, and P. T. Rumsby, Phys. Rev. Lett. **41**, 243 (1978); P. Alaterre, C. Chenais-Popovics, P. Audebert, J. P. Geindre, and J. C. Gauthier, Phys. Rev. A **32**, 324 (1985); W. H. Goldstein, R. S. Walling, J. Bailey, M. H. Chen, R. Fortner, M. Klapisch, T. Phillips, and R. E. Stewart, Phys. Rev. Lett. **58**, 2300 (1987); B. K. F. Young, R. E. Stewart, C. J. Cerjan, G. Charatis, and G. E. Busch, *ibid.* **61**, 2851 (1988); L. Zhang, S. Han, Z. Xu, Z. Zhang, P. Fan, and L. Sun, Phys. Rev. E **51**, 6059 (1995); S. H. Glenzer *et al.*, Phys. Rev. Lett. **82**, 97 (1999).
[23] Y. Hanada, K. Sugioka, Y. Gomi, H. Yamaoka, O. Otsuki, I. Miyamoto, and K. Midorikawa, Appl. Phys. A: Mater. Sci. Process. **79**, 1001 (2004).
[24] Y. Hanada, K. Sugioka, K. Obata, S. V. Garnov, I. Miyamoto, and K. Midorikawa, J. Appl. Phys. **99**, 043301 (2005).
[25] E. D. Palik, *Handbook of Optical Constants of Solids* (Academic, Orlando, 1985).
[26] S. C. Wilks, W. L. Kruer, M. Tabak, and A. B. Langdon, Phys. Rev. Lett. **69**, 1383 (1992); X. Y. Wang and M. C. Downer, Opt. Lett. **17**, 1450 (1992); A. Rousse, P. Audebert, J. P. Jeindre, F. Fallies, J.-C. Gauthier, A. Mysyrowicz, G. Grillon, and A. Antonetti, Phys. Rev. E **50**, 2200 (1994); G. Guethlein, M. E. Foord, and D. Price, Phys. Rev. Lett. **77**, 1055 (1996); S. Bastiani, A. Rousse, J. P. Jeindre, P. Audebert, C. Quoix, G. Hamoniaux, A. Antonetti, and J.-C. Gauthier, Phys. Rev. E **56**, 7179 (1997); L. A.

Gizzi, A. Guilietti, O. Willi, and D. Riley, *ibid.* **62**, 2721 (2000).
[27]R. McCluney, *Introduction to Radiometry and Photometry* (Artech House, Boston, 1994).
[28]P. H.-Y. Lee and M. D. Rosen, Phys. Rev. Lett. **42**, 236 (1979); J. R. Albritton and A. B. Langdon, *ibid.* **45**, 1794 (1980).
[29]D. F. Price, R. M. More, R. S. Walling, G. Guethlein, R. L. Shepherd, R. E. Stewart, and W. E. White, Phys. Rev. Lett. **75**, 252 (1995).
[30]S. I. Kudryashov, K. Lyon, and S. D. Allen, J. Appl. Phys. **100**, 124908 (2006).
[31]F. W. Dabby and U. C. Paek, IEEE J. Quantum Electron. **8**, 106 (1972).
[32]S. I. Anisimov, A. M. Bonch-Bruevich, M. A. El'yashevich, Ya. A. Imas, N. A. Pavlenko, and G. S. Romanov, Sov. Phys. Tech. Phys. **11**, 935 (1967); see also A. A. Samokhin, *Reports of General Physics Institute* (Moscow, Nauka, 1988), Vol. 13 (in Russian); S. I. Anisimov and V. A. Khokhlov, *Instabilities in Laser-Matter Interactions* (CRC, Boca Raton, FL, 1995).
[33]A. Miotello and R. Kelly, Appl. Phys. Lett. **67**, 3535 (1995).
[34]B. J. Garrison, T. E. Itina, and L. V. Zhigilei, Phys. Rev. E **68**, 041501 (2003).
[35]S. I. Kudryashov and S. D. Allen, J. Appl. Phys. **92**, 5627 (2002).
[36]J. Zhang, K. Sugioka, and K. Midorikawa, Appl. Phys. A: Mater. Sci. Process. **69**, S879 (1999).